Petroleum Science 19 (2022) 472–485

Contents lists available at ScienceDirect

Petroleum Science

journal homepage: www.keaipublishing.com/en/journals/petroleum-science

Original Paper

Hydrocarbon generation history constrained by thermal history and hydrocarbon generation kinetics: A case study of the Dongpu Depression, Bohai Bay Basin, China

Mei-Hua Yang [a], Yin-Hui Zuo [a, b, *], Kang-Nan Yan [a], Yong-Shui Zhou [c], Yun-Xian Zhang [c], Cheng-Fu Zhang [c]

[a] State Key Laboratory of Oil and Gas Reservoir Geology and Exploitation, Chengdu University of Technology, Chengdu, Sichuan 610059, China
[b] Energy & Geoscience Institute, University of Utah, Salt Lake City, UT, 84108, USA
[c] Research Institute of Exploration and Development, Zhongyuan Oilfield, SINOPEC, Puyang, Henan 457001, China

ARTICLE INFO

Article history:
Received 9 April 2020
Accepted 21 June 2021
Available online 22 December 2021

Edited by Jie Hao

Keywords:
Dongpu depression
Thermal history
Hydrocarbon generation kinetics
Hydrocarbon generation mode
Hydrocarbon generation history

ABSTRACT

With the increasing exploration and development of typical hydrocarbon-rich depressions, such as the Dongpu Depression, the exploitation difficulty of shallow formations is increasing. There is an urgent need to clarify the hydrocarbon generation mode and hydrocarbon generation histories in deep formations. In this study, a gold tube-autoclave closed system was used to simulate the hydrocarbon generation processes and establish the hydrocarbon generation mode of different types of kerogen. Then, constrained by the thermal history and hydrocarbon generation kinetics, hydrocarbon generation histories were modeled. The results show that hydrocarbon generation evolution can be divided into five stages, and the maturity of each stage is different. The hydrocarbon generation history of the source rocks of the Shahejie 3 Formation mainly dates from the early depositional period of the Shahejie 1 Formation to the middle depositional period of the Dongying Formation. Hydrocarbon generation history constrained by thermal history and hydrocarbon generation kinetics is more in line with actual geological conditions. Moreover, this research can provide important hydrocarbon generation parameters for deep oil and gas exploration and exploitation of the Shahejie 3 Formation in the Dongpu Depression.

1. Introduction

Hydrocarbon generation kinetics is based on the principle of chemical reaction kinetics, and a pyrolysis method under rapid heating is used in the laboratory to reproduce the process of hydrocarbon generation in source rocks under geological conditions (Ungerer and Pelet, 1987; Burnham and Sweeney, 1989; Behar et al., 1992; Pepper and Corvi, 1995; Ni et al., 2011; Li and Zhu, 2014; Abbassi et al., 2016; Shao et al., 2020). Thermal history of the sedimentary basins can help to evaluate the hydrocarbon generation history of the source rocks more comprehensively. Consequently, research on thermal history is currently an important basic work that is necessary for the evaluation of oil and gas resources in sedimentary basins.

Geochemists often use a fixed heating rate (such as 3 °C/Ma) to convert the hydrocarbon generation model obtained in the laboratory into the actual hydrocarbon generation history (Schenka and Dieckmannb, 2004; Dieckmann and Keym, 2006; Han et al., 2014). In fact, the study area has undergone complex structural evolutions, which affects the thermal state and thermal history (Zuo et al., 2020b). Therefore, the rate of temperature change during geological history is variable, especially in cases where the rift basin is more complicated. During a period of strong rifting, the heating rate can reach 10 °C/Ma (Zuo et al., 2011, 2015, 2017, 2020a, 2020a). Therefore, applying a fixed heating rate to study the hydrocarbon generation history does not accurately represent the actual geological condition. The study of the thermal history is essential when applying hydrocarbon generation kinetic parameters to the actual hydrocarbon generation history and hydrocarbon production. Moreover, different types of kerogen (DTK) have different hydrocarbon generation kinetic parameters, and there are certain

* Corresponding author. State Key Laboratory of Oil and Gas Reservoir Geology and Exploitation, Chengdu University of Technology, Chengdu, 610059, China.
E-mail address: zuoyinhui@tom.com (Y.-H. Zuo).

https://doi.org/10.1016/j.petsci.2021.10.009

differences in the maturity classification (Moattari et al., 2012; Wang et al., 2020). Therefore, it is necessary to establish the hydrocarbon generation kinetic parameters of DTK in the Dongpu Depression and determine the applicable maturity classification criteria.

The Dongpu Depression is a typical oil and natural gas rich depression in the Bohai Bay Basin, China (Fig. 1). After more than 60 years of exploration and development of the Dongpu Depression, these activities have now become more challenging. Oil and gas production has declined gradually over the years (Tang et al., 2016; Zuo et al., 2017; Jiang et al., 2019). Hence, there is an urgent need to find conventional and unconventional oil and gas resources in the deeper formations of the Dongpu Depression (>3500 m) (Tang et al., 2016; Zuo et al., 2017). Thus, the primary task is to explain the hydrocarbon generation potential, generation mode, and generation processes of the DTK in deep formations. However, these parameters have not yet been investigated well.

In this study, high-temperature and high-pressure pyrolysis experiments were conducted in a gold tube autoclave closed system. The hydrocarbon generation mode of DTK was established based on the experimental results. Combined with the thermal history and basin simulation software, this study reproduced the hydrocarbon generation history of the DTK. This work provides important parameters for determining the hydrocarbon generation characteristics and for the re-evaluation of the source rocks in the Dongpu Depression.

2. Geological settings

The Dongpu Depression is a typical hydrocarbon-rich depression in the Bohai Bay Basin and extends along the NNE strike direction with an area of approximately 5300 km^2 (Zuo et al. 2014, 2016, 2017) (Fig. 2a and b). Five formations have been deposited since the Ecocene (Feng et al., 2014), including the Shahejie, Dongying, Guantao, Minghuazhen, and Pingyuan Formations. The Shahejie 3 Formation is the main source rock of the Dongpu Depression Formation (Fig. 3) (Feng et al., 2014; Hu et al., 2018; Jiang et al., 2019). The Dongpu Depression is mainly affected by the differential activities of the three basement faults: the Lanliao, Huanghe, and Changyuan faults. From east to west, there are the Lanliao fault zone, eastern subdepression, central uplift zone, western subdepression, and western slope zone (Fig. 2a) (Zuo et al., 2017; Jiang et al., 2019; Jiang et al. 2021).

The Cenozoic tectonic evolution in the Dongpu Depression can be divided into the following four stages: (1) the initial rift stage (50–42 Ma), during which the geothermal gradient increased. The Lanliao fault zone in the eastern Dongpu Depression was strongly active, controlling the basic structure of the depression; (2) the rapid rifting stage (42–33 Ma), during which the geothermal gradient decreased rapidly. Most of the faults in the Dongpu

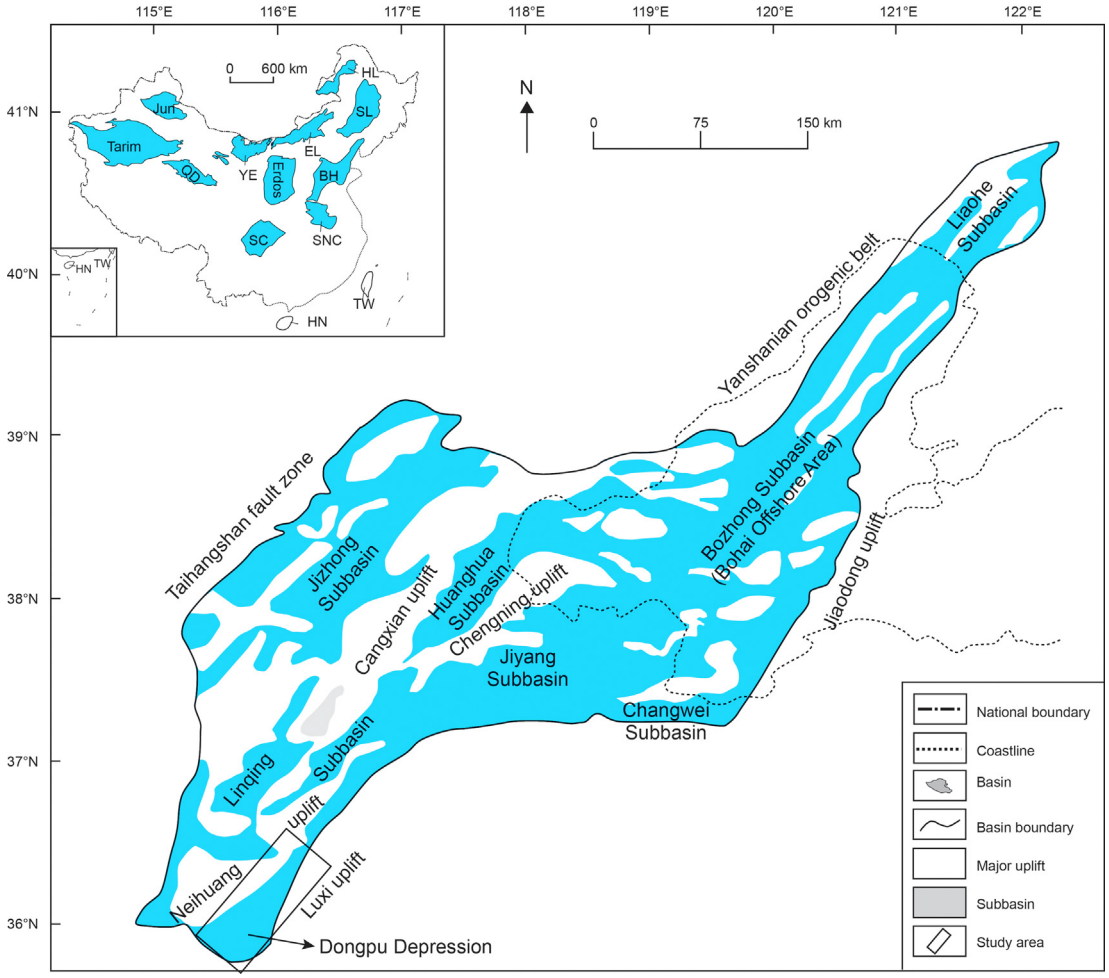

Fig. 1. Structural unit division of the Bohai Bay Basin and position of the Dongpu Depression (Zuo et al., 2017). Jun — Junggar Basin; QD — Qaidam Basin; YE — Yingen-Ejinaqi Basin; EL — Erlian Basin; HL — Hailaer Basin; SL — Songliao Basin; BH — Bohai Bay Basin; SNC — Southern part of North China Basin; SC — Sichuan Basin; HN — Hainan; TW — Taiwan.

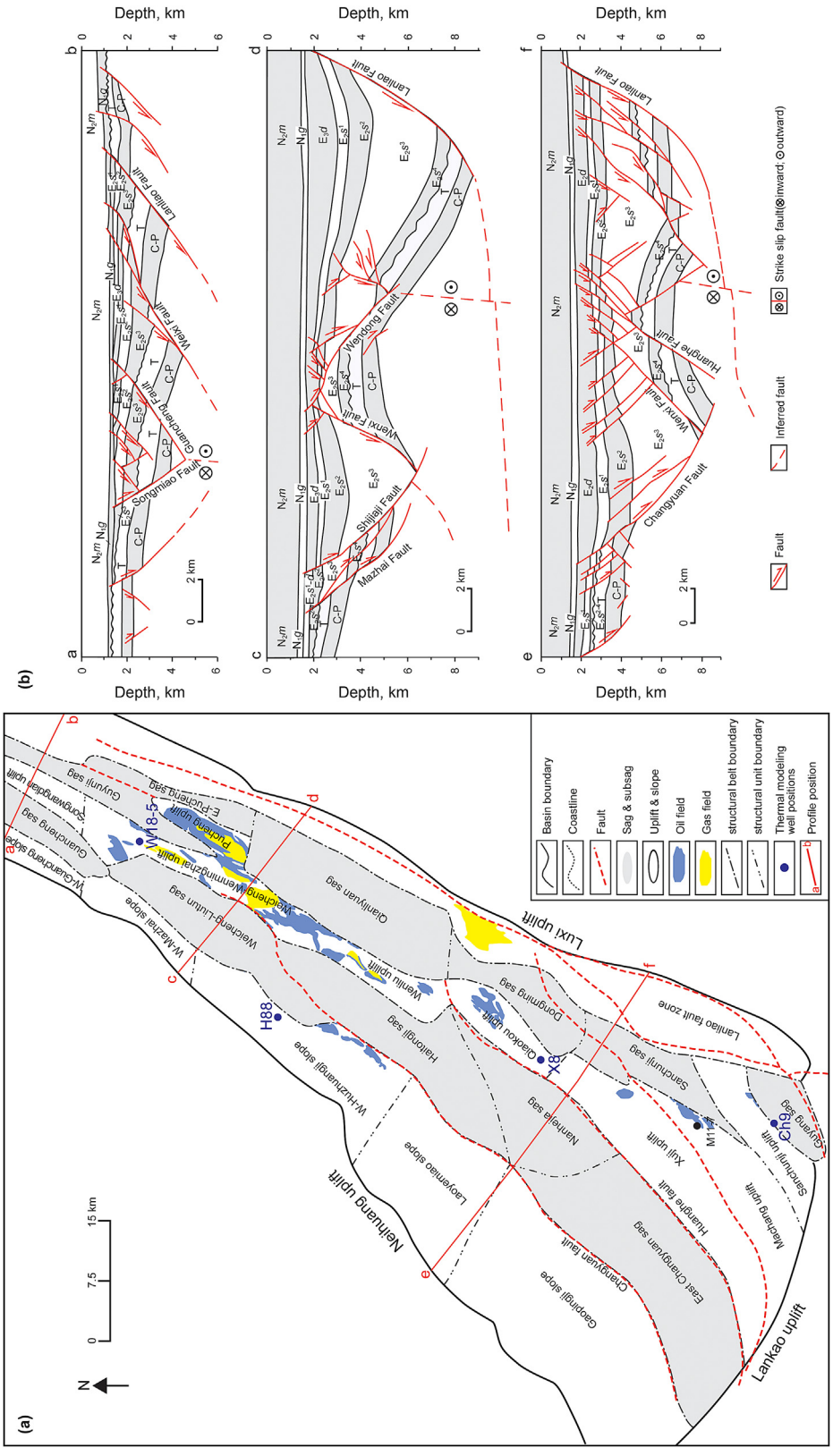

Fig. 2. (a) Structural unit division of the Dongpu Depression; (b) Structural profile (modified from Zuo et al., 2017 and Ma et al., 2017).

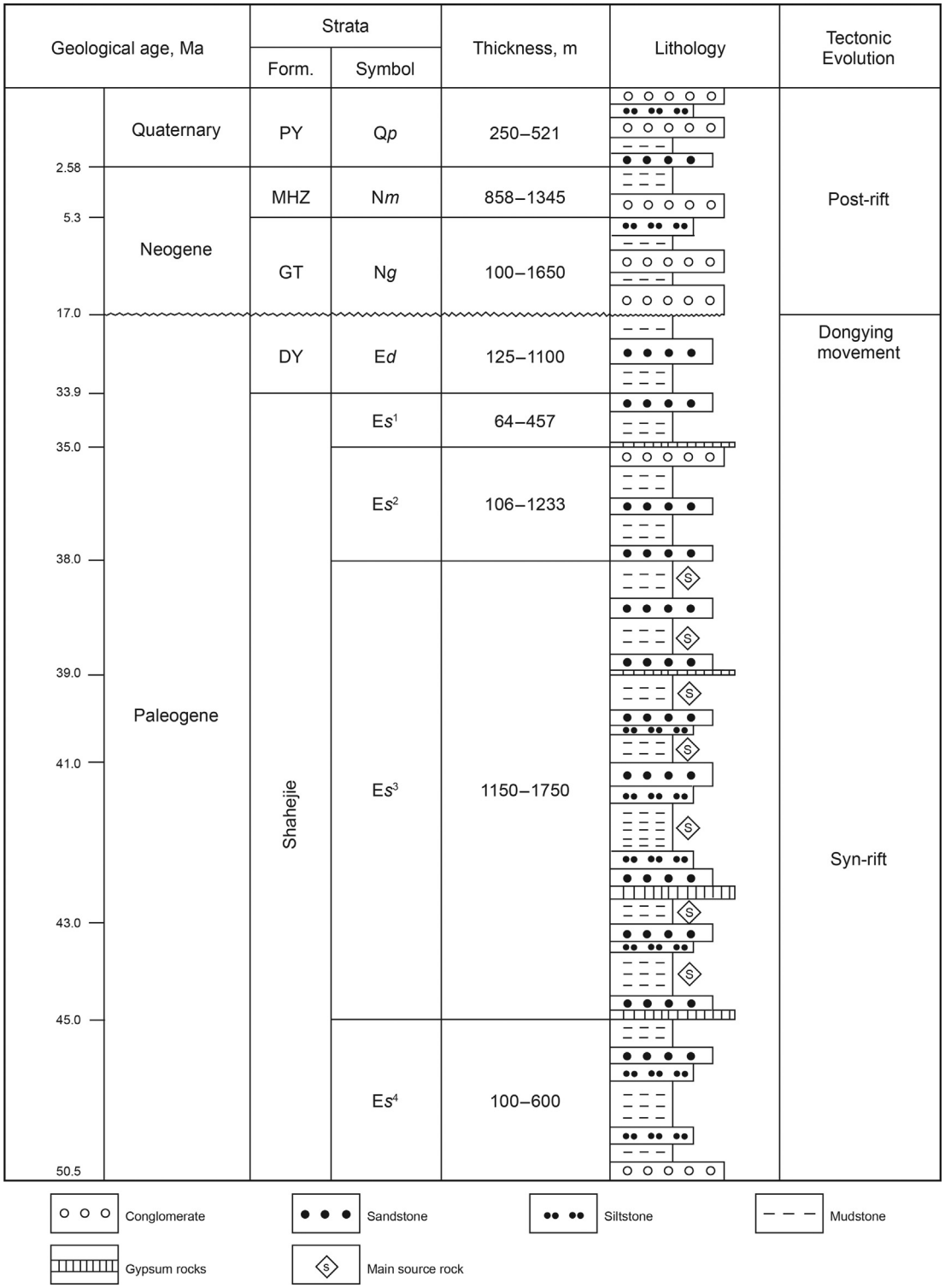

Fig. 3. Stratigraphic column map of the Dongpu Depression (Zuo et al., 2017). PY — Pingyuan Formation; MHZ — Minghuazhen Formation; GT — Guantao Formation; DY — Dongying Formation; Es — Shahejie Formation.

Depression began to move on a large scale, which caused the area to expand rapidly, increasing the thickness of the strata. Under the combined influence of the Yellow River fault zone in the center and the Lanliao fault zone in the east, the tension and tension amount of the Dongpu Depression increased, causing the other small faults to become vigorously active; (3) the late rifting stage (33–27 Ma), during which the geothermal gradient increased and the basement fault began to gradually weaken; (4) the depression stage (27–0 Ma), during which the geothermal gradient decreased. Since the Neogene, the Dongpu Depression entered the stage of slow settlement. The differential rise and fall caused by the Dongying Movement stopped, and some unconformities were formed (Fig. 4).

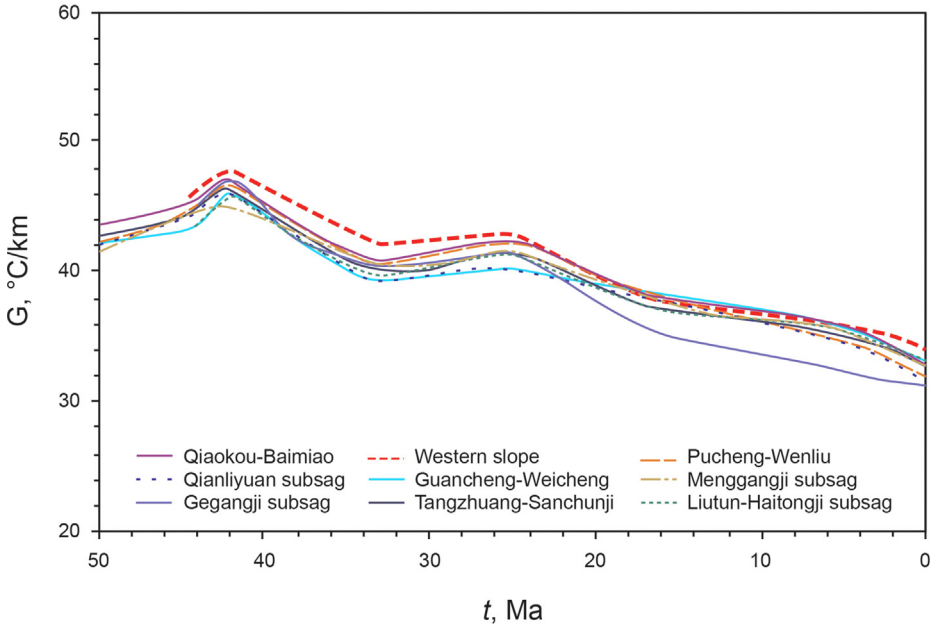

Fig. 4. Thermal gradient evolution history of the Dongpu Depression (Zuo et al., 2017).

Table 1
Organic matter abundance of the Shahejie 3 Formation source rocks in the Dongpu Depression (Jiang et al., 2019).

Structural units	TOC, %	Chloroform asphalt "A", %	HC, ppm	S_1+S_2, mg/g	Evaluation
Gegangji sag	0.04 – 3.85 0.40(508)	0.0013 – 0.7160 0.0409(157)	0.75 – 1364.52 56.72(486)	0.001 – 16.440 0.683(486)	Poor - non source rock
Qianliyuan sag	0.02 – 6.51 0.61(2753)	0.0002 – 1.4153 0.1267(574)	1.33 – 50820.90 1941.61(1487)	0.002 – 61.230 2.339(1487)	Medium-good source rock
Menggangji sag	0.04 – 1.31 0.40(170)	0.0013 – 0.1681 0.0278(24)	1.08 – 1784.50 352.07(92)	0.001 – 2.150 0.424(92)	Poor - non source rock
Haitongji - Liutun sag	0.04 – 8.51 0.80(978)	0.0004 – 1.9308 0.1776(284)	1.08 – 56135.00 2272.82(576)	0.001 – 68.450 2.738(576)	Medium-good source rock

TOC — Total organic carbon; HC — Total hydrocarbon content; S_1+S_2 — Hydrocarbon generation potential.

Table 2
Source rock samples of the Shahejie 3 Formation in the Dongpu Depression.

Location	Well No.	Lithology	Depth, m	R_o, %	TOC, %	Kerogen type
Weicheng-Wenmingzhai uplift	W18-5	Gray mudstone	2780.68	0.56	4.45	I
Guyang sag	Ch9	Gray mudstone	2500.80	0.73	1.05	II_1
W-Huzhuangji slope	H88	Gray mudstone	1456.80	0.45	0.83	II_2
Qiaokou uplift	X8	Dark gray mudstone	3156.80	0.85	0.39	III

TOC — Total organic carbon; R_o — Vitrinite reflectance.

The present geothermal gradient in the Dongpu Depression is 20.0–56.5 °C/km with an average of 34.8 °C/km. The terrestrial heat flow is 37.8–106.8 mW/m^2, with an average of 66.8 mW/m^2. Therefore, the Dongpu Depression is characterized by a medium geothermal field between the stable tectonic zone and the active tectonic zone (Zuo et al., 2017). The Dongpu Depression experienced two high peaks of heat flow; one during the middle sedimentary stage of the Shahejie 3 Formation and the other during middle sedimentary stage of the Dongying Formation. Moreover, the heat flow of the former was larger than that of the latter, and the maximum heat flow values were 70.5–77.5 mW/m^2 and 64.8–70.0 mW/m^2, respectively (Fig. 4) (Li et al., 2016; Zuo et al., 2017; Tang et al., 2019).

3. Methods and principles

3.1. Gold tube-autoclave closed system and pyrolysis samples

The experiments were carried out at the Guangzhou Institute of Geochemistry, Chinese Academy of Sciences. The gold tube-autoclave closed system was chosen to reproduce the hydrocarbon generation of the source rocks. The applied fluid pressure and maximum temperature of the system were 100 MPa and 600 °C, respectively. In this experiment, the first step was to extract kerogen from the source rocks. The pressure was set to 50 MPa, and the extracted kerogen sample was heated from 250 °C to 600 °C at heating rates of 2 °C/h and 20 °C/h. The temperature fluctuations and pressure errors were controlled within 1 °C and 0.1 MPa, respectively.

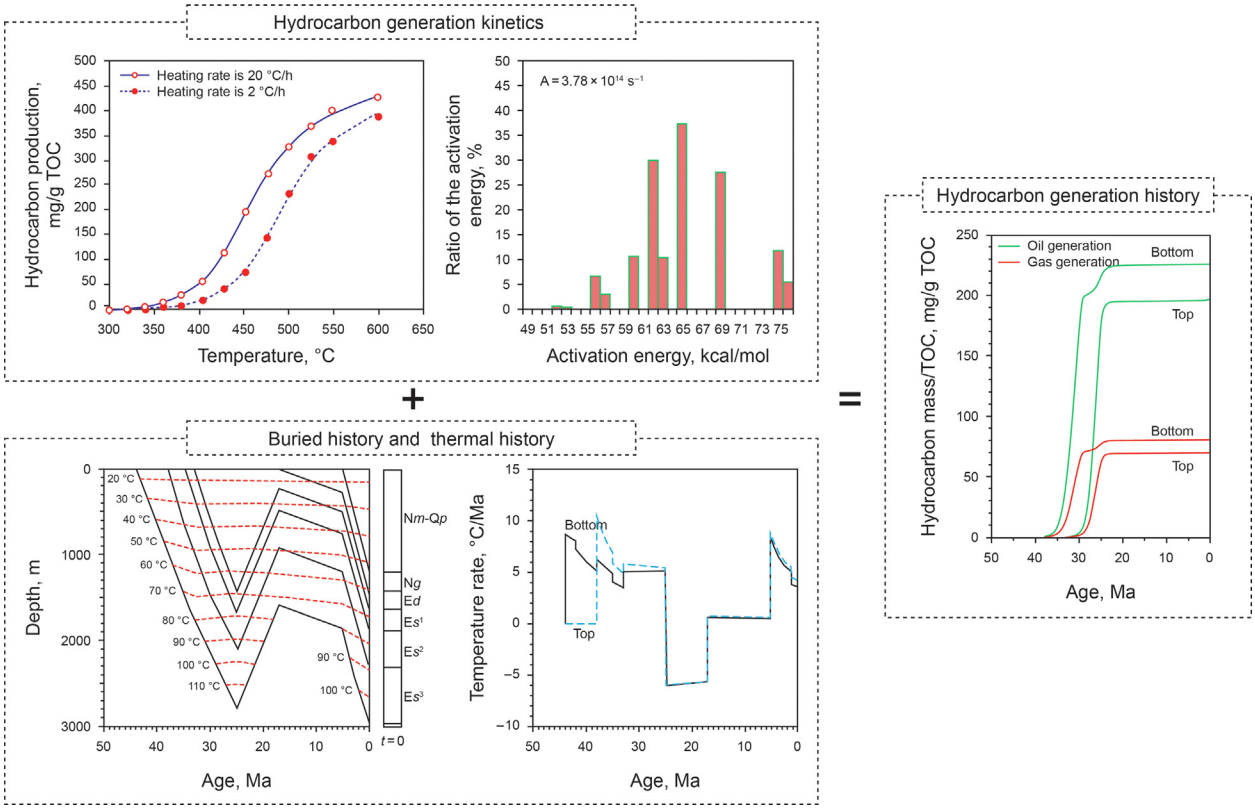

Fig. 5. Hydrocarbon generation history research method.

The Shahejie 3 Formation has the most important source rocks in the Dongpu Depression, and dark mudstones are mainly distributed in the Haitongji-Liutun and Qianliyuan areas. The source rocks are comprehensively evaluated as medium-good source rocks (Table 1), which are mainly type III-II and type I, and the greatest thickness of dark mudstone exceeds 2200 m and 2000 m, respectively (Jiang et al., 2019). Moreover, kerogen with low maturity can be used to obtain a complete series of hydrocarbon generation through hydrocarbon generation pyrolysis simulations (Peters et al., 2015; Lee et al., 2016; Yan et al., 2019; Yousif et al., 2019). Therefore, in this study, we selected four DTK samples from the Shahejie 3 Formation of the Dongpu Depression to conduct a high-temperature and high-pressure pyrolysis experiment utilizing a gold tube autoclave closed system (Table 2).

Table 3
Rock thermal conductivity for strata in the Dongpu Depression (Zuo et al., 2014).

Strata	Lithology	Sample No.	Rock thermal conductivity, W/(m·K)	Average rock thermal conductivity, W/(m·K)	Stratum thermal conductivity, W/(m·K)
Ed	Siltstone	3	1.42–2.79	2.16	2.20
	Mudstone	1	2.22	2.22	
Es_1	Limestone	1	2.05	2.05	1.85
	Siltstone	1	2.12	2.12	
	Mudstone	2	1.48–2.08	1.78	
Es_2	Dolomite	1	1.98	1.98	2.02
	Siltstone	68	1.36–3.06	2.16	
	Mudstone	38	1.25–2.77	1.97	
	Salt rock	1	2.67	2.67	
Es_3^1	Dolomite	1	2.26	2.26	1.76
	Siltstone	26	1.34–2.48	1.88	
	Mudstone	33	1.12–2.47	1.72	
	Salt rock	1	2.49	2.49	
Es_3^2	Conglomerate	1	1.76	1.76	1.84
	Siltstone	7	1.73–2.88	2.40	
	Mudstone	8	1.24–2.19	1.65	
Es_3^3	Sandstone	3	1.07–3.14	2.26	1.95
	Siltstone	39	1.58–3.13	2.21	
	Mudstone	28	1.16–2.64	1.85	
Es_3^4	Siltstone	15	1.47–3.22	2.27	2.01
	Mudstone	13	1.27–2.42	1.84	
Es_4	Sandstone	3	1.94–2.46	2.26	2.18
	Siltstone	19	1.34–3.12	2.40	
	Mudstone	9	1.60–2.49	2.09	
	Salt rock	1	2.51	2.51	

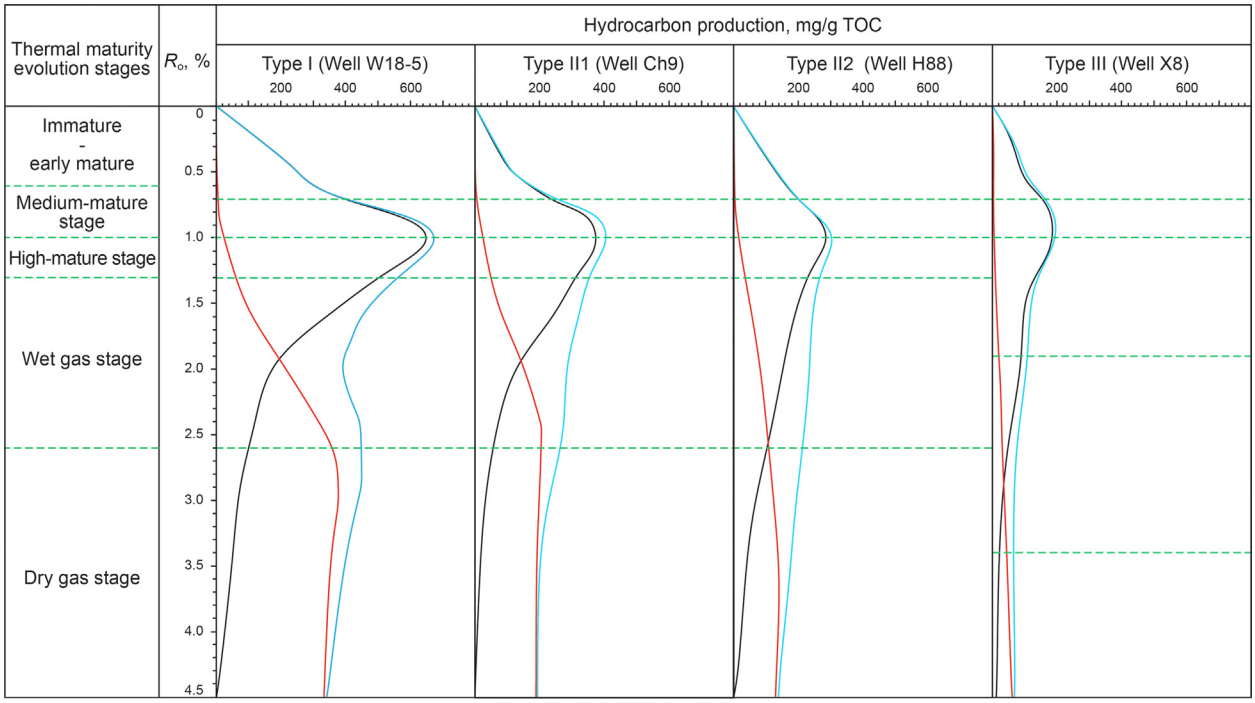

Fig. 6. Thermal maturity evolution stages of the Dongpu Depression. Black line: C_{6+}; red line: $C_{1\text{-}5}$; blue line: total hydrocarbon.

3.2. Hydrocarbon generation history research method based on thermal history and hydrocarbon generation kinetics

Samples with DTK were selected to conduct high-temperature and high-pressure pyrolysis experiments in a gold tube-autoclave closed system (Table 2). The activation energy and pre-exponential factors were obtained based on hydrocarbon generation kinetics using the software KINETICS and hydrocarbon production. Subsequently, combined with the thermal history and hydrocarbon generation kinetic parameters, the software Basin-Mod 1D was used to simulate the hydrocarbon generation history of the four types of kerogen (Fig. 5).

Table 4
Kinetic parameters of hydrocarbon generation in the Dongpu Depression.

Kerogen type	Primary cracking			Secondary cracking		
	Initial HC potential	Activation energy, kcal/mol	Arrhenius constant, s^{-1}	Initial HC Potential	Activation energy, kcal/mol	Arrhenius constant, s^{-1}
Type I (W18-5)	0.121	48	5.50×10^{15}	1	65	3.78×10^{14}
	0.185	49	5.50×10^{15}			
	0.041	53	5.50×10^{15}			
	0.183	56	5.50×10^{15}			
	0.419	57	5.50×10^{15}			
	0.044	60	5.50×10^{15}			
	0.005	61	5.50×10^{15}			
	0.003	62	5.50×10^{15}			
Type II_1 (Ch9)	0.096	50	3.50×10^{16}	1	58	7.50×10^{12}
	0.144	51	3.50×10^{16}			
	0.139	55	3.50×10^{16}			
	0.449	58	3.50×10^{16}			
	0.118	59	3.50×10^{16}			
	0.055	62	3.50×10^{16}			
Type II_2 (H88)	0.273	41	2.80×10^{11}	1	50	6.50×10^{10}
	0.0173	42	2.80×10^{11}			
	0.293	45	2.80×10^{11}			
	0.159	46	2.80×10^{11}			
	0.173	48	2.80×10^{11}			
	0.086	49	2.80×10^{11}			
Type III (X8)	0.165	47	5.50×10^{14}	1	46	2.41×10^{9}
	0.032	48	5.50×10^{14}			
	0.226	51	5.50×10^{14}			
	0.505	52	5.50×10^{14}			
	0.047	55	5.50×10^{14}			
	0.019	56	5.50×10^{14}			
	0.006	58	5.50×10^{14}			

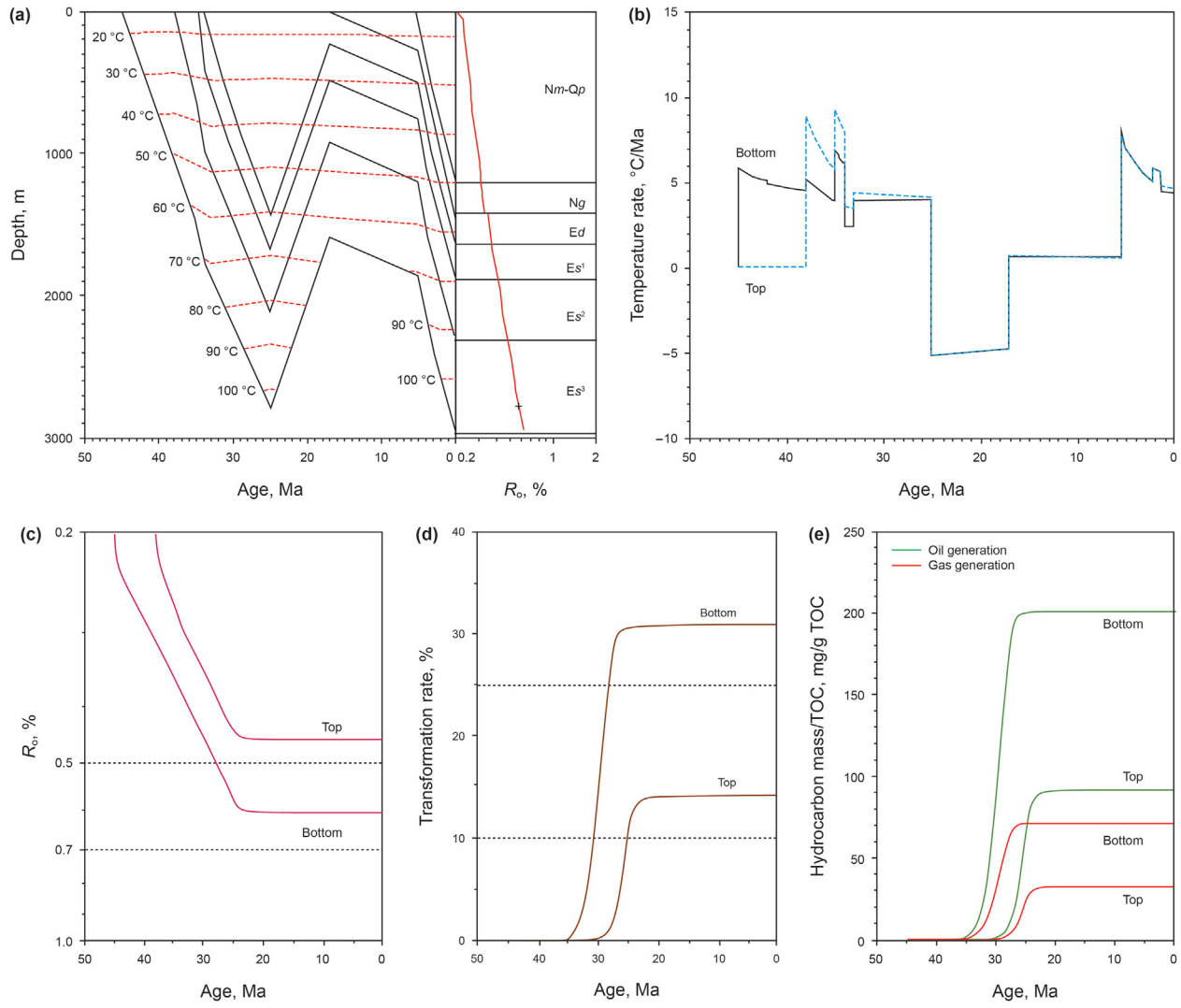

Fig. 7. Buried history, thermal history, maturity history and hydrocarbon generation history of well W18-5 (Type I kerogen) in the Shahejie 3 Formation. (a) Buried history and thermal history; (b) Temperature rate; (c) Maturity history; (d) Transformation rate; (e) Hydrocarbon generation history.

3.3. The correction of the hydrocarbon generation mode

The classic hydrocarbon generation mode assumes that the vitrinite reflectance value of the oil peak of the four types of kerogen is 1.0% (Tissot et al., 1987). In the closed experimental system, the constant pressure of 50 MPa applied during the experiment caused the peak of oil generation to arrive early (Kuske et al., 2019). Therefore, the vitrinite reflectance value of the simulated temperature should be corrected before dividing the hydrocarbon generation mode. In response to this phenomenon, Gao et al. (2005) proposed a proportional correction method to make the simulation results more consistent with the actual geological conditions. It is assumed that the differences in the R_o values under each simulated temperature point are consistent with those under actual geological conditions. Therefore, the oil production peak of pyrolysis corresponds to that under actual geological conditions. The vitrinite reflectance of the oil peak was corrected to 1.0%, and the vitrinite reflectance values of the other simulated temperature points were corrected to the corresponding values by a certain ratio (Gao et al., 2005). Therefore, in this study, the proportional correction method was chosen to correct the vitrinite reflectance value before dividing the hydrocarbon generation mode.

3.4. Basic parameters and constraints

The basic parameters required in the simulation included the amount of denudation during critical geological periods, lithological parameters, stratigraphy, geochemical parameters of the source rocks, surface temperature, present geothermal field, thermal history, and thermal properties of the rocks. Data on the stratigraphy, lithologic parameters, and geochemical parameters of the source rocks were provided for the Zhongyuan Oilfield. Table 3 shows the erosion and rock thermal conductivity during geological periods (Zuo et al., 2017). The age at the bottom of each formation is shown in Fig. 3.

4. Results

4.1. Hydrocarbon generation mode

By analyzing the products of the DTK samples from the Dongpu Depression, the hydrocarbon generation mode was divided into five thermal evolution stages in this study based on the variation regularity in hydrocarbon production (Fig. 6). (1) Immature-early maturity stage: R_o<0.7%. Because the initial maturity of the samples was high, the experimental products in this stage were lacking.

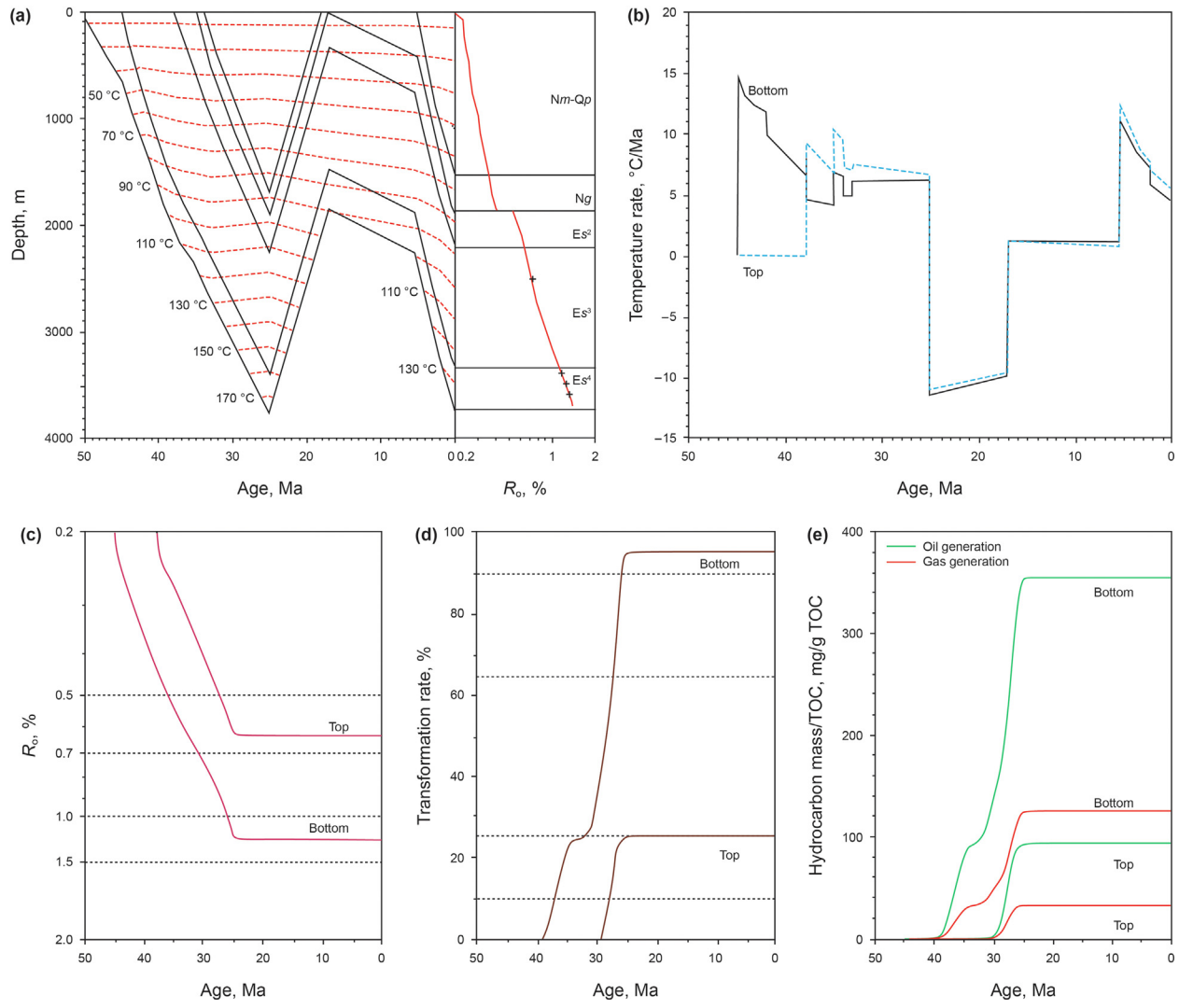

Fig. 8. Buried history, thermal history, maturity history and hydrocarbon generation history of well Ch9 (Type II_1 kerogen) in the Shahejie 3 Formation. (a) Buried history and thermal history; (b) Temperature rate; (c) Maturity history; (d) Transformation rate; (e) Hydrocarbon generation history.

(2) Medium-maturity stage: $0.7\% \leq R_o < 1.0\%$. At this stage, mainly oil was generated. When R_o was 1.0%, hydrocarbon production reached its peak. (3) High-maturity stage: Types I, II_1, and II_2 kerogen reached $1.0\% \leq R_o < 1.3\%$, and type III kerogen reached $1.0\% \leq R_o < 1.9\%$. At this stage, the oil was cracked to generate a small amount of gas. (4) Wet gas stage: Types I, II_1, and II_2 kerogen reached $1.3\% \leq R_o < 2.6\%$, and type III kerogen reached $1.9\% \leq R_o < 3.4\%$. A large amount of oil was cracked to generate wet gas. (5) Dry gas stage: Types I, II_1, and II_2 kerogen reached $R_o \geq 2.6\%$, and type III kerogen reached $R_o \geq 3.4\%$. Oil production rapidly decreased to 0 mg/g total organic carbon (TOC), and the wet gas cracked to generate methane.

Oil and gas generation is a process of continuous dehydrogenation and decarbonization of organic macromolecules. Owing to the high temperature and high pressure in the closed system for pyrolysis, the system reaches the temperature required for hydrocarbon generation in a short time. However, the bonds during kerogen pyrolysis cannot be broken in a short time. Therefore, oil was generated in the experimental system when R_o>2.0%.

4.2. Hydrocarbon generation kinetic parameters of the different types of kerogen

Based on the results of the pyrolysis experiments and the hydrocarbon generation kinetic parameters, this research explained the hydrocarbon generation kinetic characteristics of the DTK in the Dongpu Depression (Table 4). The results showed that during the primary cracking, that is, the pyrolysis of kerogen, the dominant activation energies of type I and type II_1 kerogen were much higher than those of the other two, and more energy was required for cracking. During the secondary cracking, that is, the cracking of hydrocarbons produced in earlier stages, the better kerogen type had a higher activation energy and larger pre-exponential factor, and more energy was required. The hydrocarbons generated by type III kerogen were more prone to cracking, and type II_1 and type II_2 kerogen had characteristics that were between those of type I and type III kerogen.

Well W18-5 was taken as an example. The paleotemperature of well W18-5 reached its maximum in the middle sedimentary stage of the Dongying Formation. The maximum paleotemperature at the

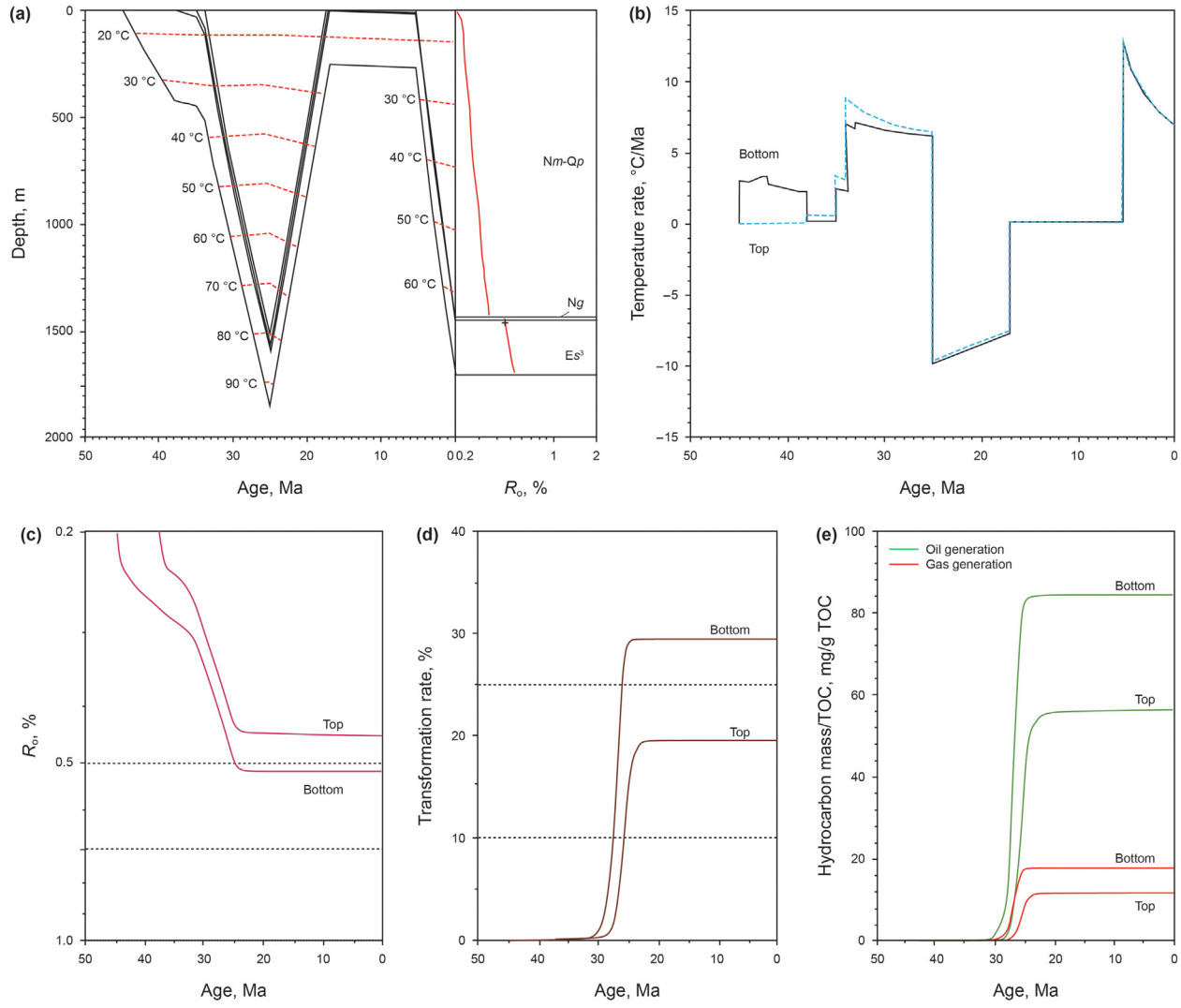

Fig. 9. Buried history, thermal history, maturity history and hydrocarbon generation history of well H88 (Type II_2 kerogen) in the Shahejie 3 Formation. (a) Buried history and thermal history; (b) Temperature rate; (c) Maturity history; (d) Transformation rate; (e) Hydrocarbon generation history.

bottom of the Shahejie 3 Formation was higher than 10 °C (Fig. 7a). Fig. 7b shows the relationship between the temperature change rate and geological time, revealing that the well experienced complicated temperature increases and reductions. At 38 Ma, the maximum heating rate reached 10 °C/Ma, and at 25 Ma, the cooling rate reached 5 °C/Ma (Fig. 7b). The maturity evolution simulation results showed that the top and bottom of the source rocks reached their maximum maturity at 22 Ma, which were 0.46% and 0.61%, respectively; their maturity did not increase thereafter (Fig. 7c). The simulation results of the hydrocarbon transformation rate showed that the current transformation rate of the source rocks is 14%–31%, which is a rather low transformation rate (Fig. 7d). The hydrocarbon generation process of the bottom source rock was from the early depositional period of the Shahejie 1 Formation to the middle depositional period of the Dongying Formation (35–25 Ma). The hydrocarbon generation process of the top source rock occurred during the middle depositional period of the Dongying Formation (30–22 Ma). The maximum oil and gas generated mass were 91.09–200.44 mg/g TOC and 33.11–70.66 mg/g TOC, respectively (Fig. 7e).

The remaining simulation results are shown in Figs. 8–10 and Table 5. Among them, the bottom source rock of well Ch9 has two stages of hydrocarbon generation and has reached an over-mature stage at the present day. The transformation rate of the bottom source rock is more than 90%, while the top source rock transformation rate is below 30%. The source rock of well H88 has a low maturity, and the transformation rate is lower than 30%. The source rock of well X8 has two stages of hydrocarbon generation and currently has reached the over-maturity stage. The transformation rate of the source rock has reached 93–100%.

5. Discussion

5.1. Comparison of hydrocarbon generation history of the same kerogen based on constant heating rate and actual heating rate

Geochemists often use the fixed heating rate of sedimentary basins (3 °C/Ma) to study the hydrocarbon generation history of source rocks. Well T8 of the Menggangji Sag in the Dongpu Depression was considered as an example (Fig. 11). The Shahejie 3 Formation is the main source rock of well T8, which is a type III kerogen. Thus, the hydrocarbon generation kinetic parameters of type III kerogen were applied to simulate the hydrocarbon generation history of well T8 based on the heating rate of 3 °C/Ma and the actual heating rate (Fig. 11, Table 4).

The formation temperature was related to the tectonic evolution

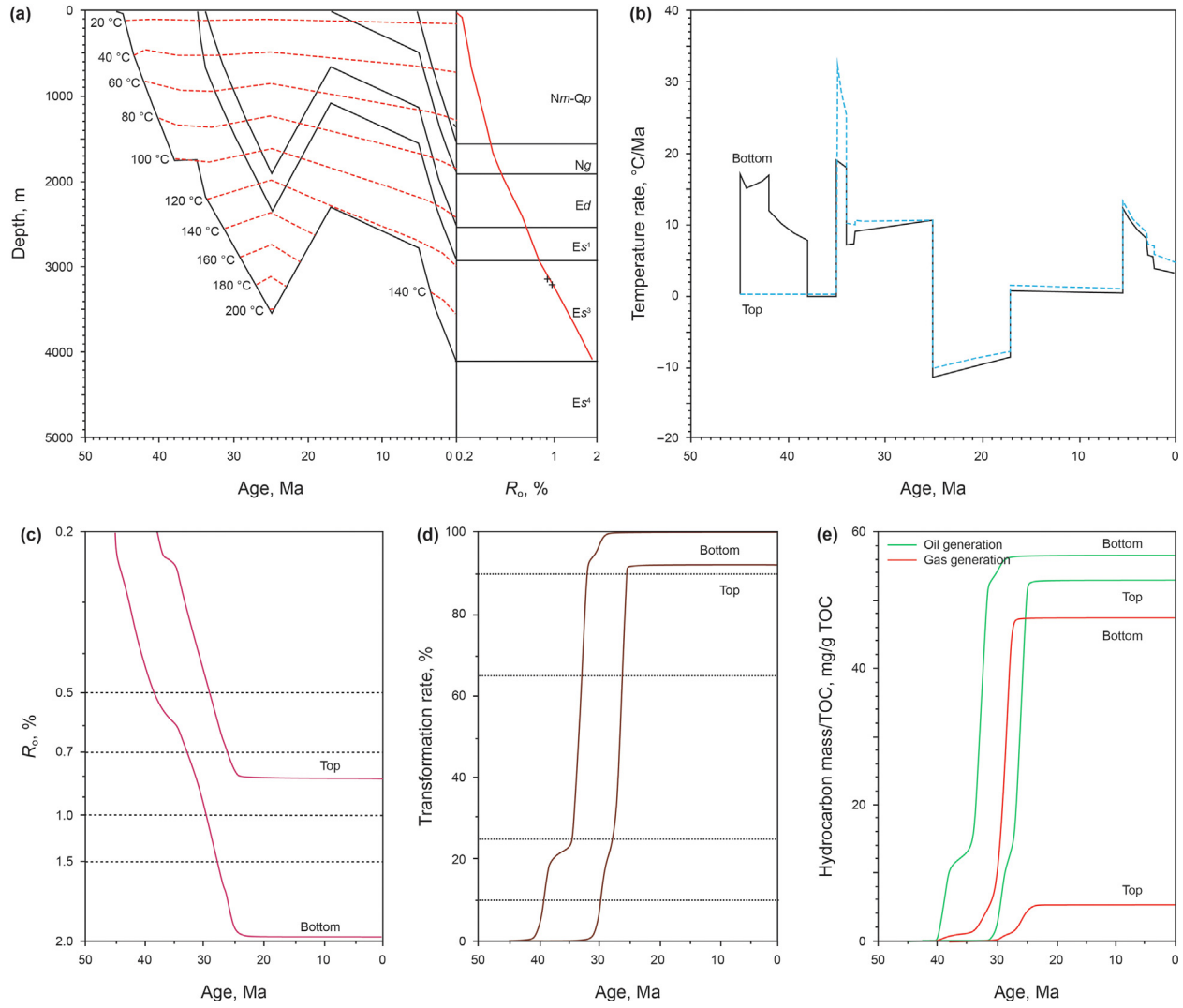

Fig. 10. Buried history, thermal history, maturity history and hydrocarbon generation history of well X8 (Type III kerogen) in the Shahejie 3 Formation. (a) Buried history and thermal history; (b) Temperature rate; (c) Maturity history; (d) Transformation rate; (e) Hydrocarbon generation history.

stages. The Cenozoic tectonic evolution in the Dongpu Depression can be divided into the following four stages: (1) the initial rift stage (50–42 Ma), during which the stratum continued to deposit and the temperature continued to rise, (2) the rapid rifting stage (42–33 Ma), during which the formation temperature increased rapidly; (3) the late rifting stage (33–27 Ma), during which the formation was uplifted and subjected to denudation, and the formation temperature decreased; and (4) the depression stage (27–0 Ma), during which the formation temperature increased slightly. In summary, combined with the structural evolution of the Dongpu Depression, it can be concluded that the formation temperature is not constant; heating and cooling processes are involved. However, according to the fixed heating rate, the strata should be a process of continuous deposition without strata uplift, which is not consistent with the actual geological conditions. Therefore, the simulated hydrocarbon generation history under the wrong temperature curve is incorrect and does not match the actual condition (Fig. 11).

The historical temperature and hydrocarbon generation history simulated at 3 °C/Ma were inconsistent with the actual condition and the thermal history of the Dongpu Depression. However, the historical maximum temperature in well T8 was similar to the present temperature of approximately 170 °C. Therefore, the hydrocarbon mass of the unit TOC calculated at the two heating rates was similar, but the hydrocarbon generation history was considerably different (Fig. 11c, f). Therefore, the application of the pyrolysis simulation results to actual geological conditions at a constant temperature heating rate is erroneous; it is necessary to simulate the hydrocarbon generation history based on the thermal history.

5.2. Comparison of hydrocarbon generation history of the different types of kerogen

DTK have different burial histories and thermal histories, hence, it is not possible to simply compare the simulation results presented above when comparing the hydrocarbon generation potential of DTK (Saad et al., 2020; Zheng et al., 2021). Based on paleotemperature data, basic geological data, and geochemical parameters of type I kerogen (well W18-5), this study compared the hydrocarbon generation histories of the four types of kerogen using different kinetic parameters of the kerogen and hydrogen indexes (Fig. 12). The results showed that the hydrocarbon generation histories of the four types of kerogen were mainly from the early depositional period of the Shahejie 1 Formation to the middle depositional period of the Dongying Formation. Among the four

Table 5
Hydrocarbon generation in the Shahejie 3 Formation in the Dongpu Depression.

Kerogen type	Well No.	Easy % R_o, %	Transformation rate, %	Oil generated mass, mg/g TOC	Gas generated mass, mg/g TOC
I	W18-5	0.46–0.61	14–31	91.09–200.44	33.11–70.66
II_1	Ch9	0.63–1.14	25–95	94.09–353.38	32.96–125.71
II_2	H88	0.45–0.51	20–29	55.93–84.66	11.66–17.99
III	X8	0.80–1.96	93–100	53.01–56.49	5.26–47.32

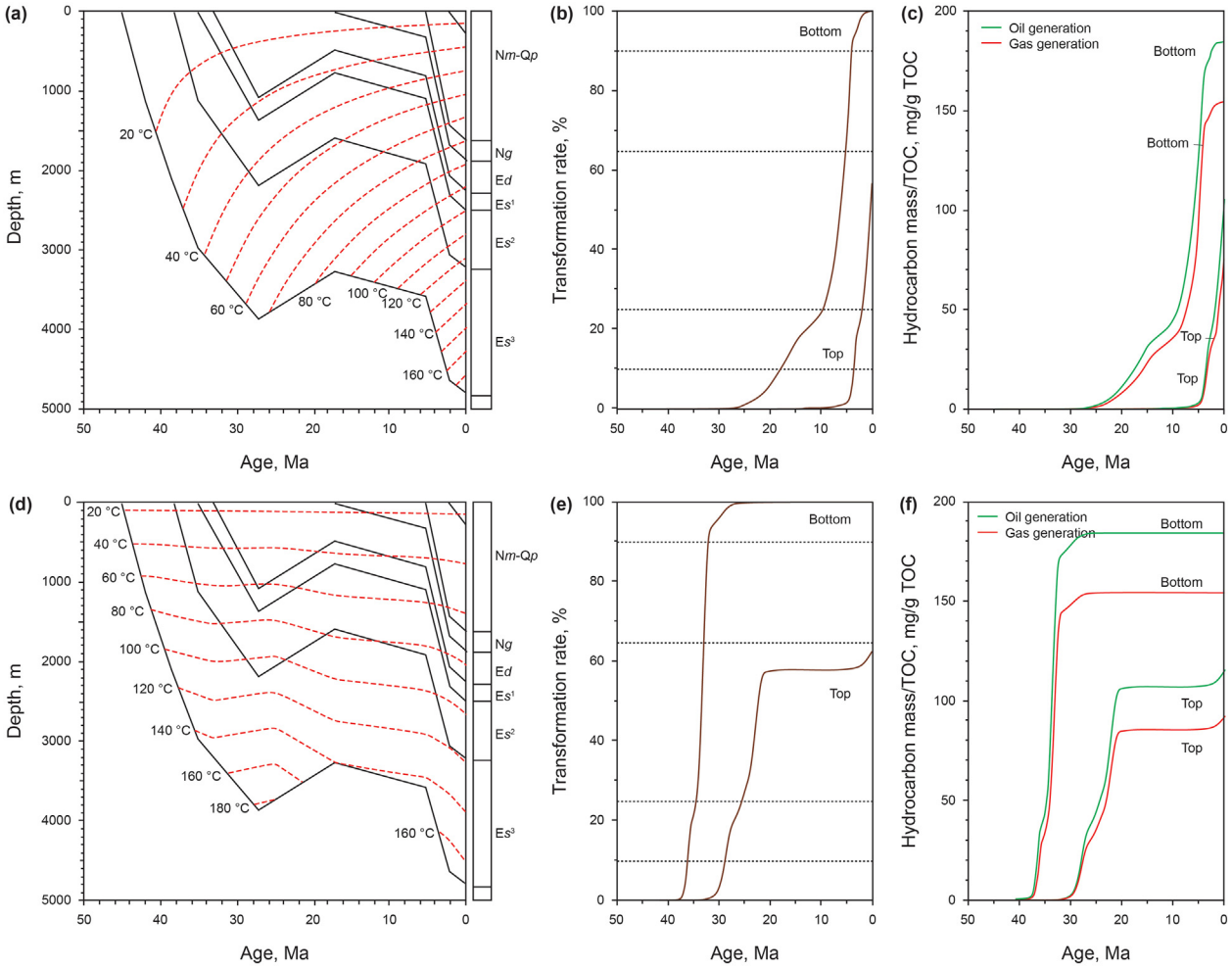

Fig. 11. Comparison of hydrocarbon generation history of well T8 based on constant heating rate (3 °C/Ma) and actual heating rate. (a) Buried history and thermal history based on 3 °C/Ma; (b) Transformation rate based on 3 °C/Ma; (c) Hydrocarbon generation history based on 3 °C/Ma; (d) Buried history and thermal history based on actual heating rate; (e) Transformation rate actual heating rate; (f) Hydrocarbon generation history actual heating rate.

types of kerogen, the hydrocarbon generation rate of type II_2 and type III kerogen reduced during 28–25 Ma.

5.3. Advantages of hydrocarbon generation history constrained by thermal history and hydrocarbon generation kinetics

The hydrocarbon generation kinetic method is based on the organic matter composition structure and chemical reaction kinetics (Wang et al., 2011; Chen et al., 2017). There are no empirical parameters. Therefore, based on the kerogen pyrolysis experiments on certain source rocks in certain basins, the hydrocarbon generation kinetic parameters of a specific kerogen type are more consistent with the actual situation.

In this study, the hydrocarbon generation mode of DTK in the Dongpu Depression was established for the first time. Furthermore, by combining thermal history with hydrocarbon generation kinetic parameters, the temperature change rate of typical wells was revised, making the simulated conditions consistent with the actual geological conditions. Considering the above two constraints, the basin simulation software BasinMod 1D was used to simulate the hydrocarbon generation history. Therefore, the study of hydrocarbon generation history constrained by thermal history and hydrocarbon generation kinetics can more accurately describe the hydrocarbon generation process of the sedimentary basins, making the simulated hydrocarbon generation history more realistic and reliable.

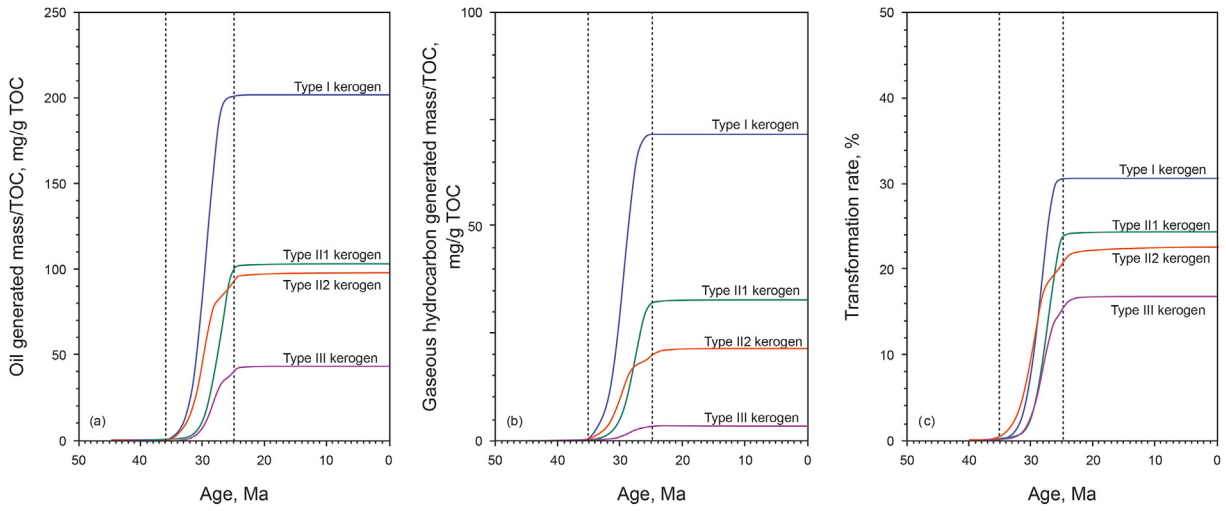

Fig. 12. Comparison of the hydrocarbon generation potentials of different types of kerogen. (a) oil potential; (b) gaseous hydrocarbon potential; (c) transformation rate.

6. Conclusions

(1) This study established the hydrocarbon generation mode of DTK in the Dongpu Depression. The hydrocarbon generation evolution can be divided into five stages, but the corresponding maturity levels of the DTK exhibit certain differences. The stages are as follows: the immature-early maturity stage with R_o<0.7%; the medium-maturity stage with 0.7% $\leq$ R_o<1.0%, the stage where the kerogen has reached peak oil production, and R_o is 1.0%; the high-maturity stage, where types I, II_1, and II_2 kerogen reached 1.0% $\leq$ R_o<1.3%, and type III kerogen reached 1.0% $\leq$ R_o<1.9%; the wet gas stage, where types I, II_1, and II_2 kerogen reached 1.3% $\leq$ R_o<2.6%, and type III kerogen reached 1.9% $\leq$ R_o<3.4%; and the dry gas stage, where types I, II_1, and II_2 kerogen reached $R_o \geq$ 2.6%, and type III kerogen reached $R_o \geq$ 3.4%.

(2) The simulation results of the hydrocarbon generation history using a fixed heating rate show the thermal history, transformation rate, and hydrocarbon generation history results that are quite different from the actual geological conditions. Therefore, the fixed heating rate cannot be used to apply the hydrocarbon generation pyrolysis simulation results to actual geological conditions.

(3) This study proposed a new method to simulate the hydrocarbon generation history based on thermal history and hydrocarbon generation kinetics and applied it to the Dongou Depression. The hydrocarbon generation histories of the four types of kerogen were mainly from the early depositional period of the Shahejie 1 Formation to the middle depositional period of the Dongying Formation.

Acknowledgements

This work was funded by the National Major Science and Technology Projects of China (Grant No. 2016ZX05006-004), the Sichuan Youth Science and Technology Foundation (Grant No. 2016JQ0043), and the National Natural Science Foundation of China (Grant No. 41972144). Our sincerest gratitude also goes to Prof. Jinzhong Liu, Dr. Song Rao, and Dr. Yan Liu for their guidance and helpful suggestions during the research.

References

Abbassi, S., Edwards, D.S., George, S.C., et al., 2016. Petroleum potential and kinetic models for hydrocarbon generation from the upper cretaceous to paleogene latrobe group coals and shales in the gippsland basin, Australia. Org. Geochem. 91, 54–67. https://doi.org/10.1016/j.orggeochem.2015.11.001.

Behar, F., Kressmann, S., Rudkiewicz, J.L., 1992. Experimental simulation in a confined system and kinetic modelling of kerogen and oil cracking. Org. Geochem. 19, 173–189. https://doi.org/10.1016/0146-6380(92)90035-V.

Burnham, A.K., Sweeney, J.J., 1989. A chemical kinetic model of vitrinite maturation and reflectance. Geochem. Cosmochim. Acta 53 (10), 2649–2657. https://doi.org/10.1016/0016-7037(89)90136-1.

Chen, Z.H., Liu, X.J., Guo, Q.L., et al., 2017. Inversion of source rock hydrocarbon generation kinetics from Rock-Eval data. Fuel 194, 91–101. https://doi.org/10.1016/j.fuel.2016.12.052.

Dieckmann, V., Keym, M., 2006. A new approach to bridge the effect of organofacies variations on kinetic modelling and geological extrapolations. Org. Geochem. 37, 728–739. https://doi.org/10.1016/j.orggeochem.2005.12.008.

Feng, Z.D., Cheng, X.S., Fu, X.L., et al., 2014. Neotectonic movements in the Dongpu depression and their controls on hydrocarbon accumulation in shallow reservoirs. Sediment. Geol. Tethyan Geol. 34 (1), 8–13 (in Chinese with English abstract).

Gao, G., Liu, G.D., Wang, Z.F., 2005. Correction of results from hydrocarbon genrating simulation. Xinjing Pet. Geol. 26 (2), 202–205 (in Chinese with English abstract).

Han, S.B., Horsfield, B., Zhang, J.C., et al., 2014. Hydrocarbon generation kinetics of lacustrine yanchang shale in southeast ordos basin, north China. Energy Fuels 28, 5632–5639. https://doi.org/10.1021/ef501011b.

Hu, H.J., Jiang, Y.L., Liu, J.D., et al., 2018. Gas generation evolution and potential analysis of carboniferous–permian coal–measured source rocks in dong depression. Earth Sci. 43 (2), 610–621. https://doi.org/10.3799/dqkx.2017.604.

Jiang, S., Zuo, Y.H., Yang, M.H., et al., 2021. Reconstruction of the Cenozoic tectono-thermal history of the Dongpu Depression, Bohai Bay Basin, China: constraints from apatite fission track and vitrinite reflectance data. J. Petrol. Sci. Eng. 205, 108809. https://doi.org/10.1016/j.petrol.2021.108809.

Jiang, Z.R., Zuo, Y.H., Yang, M.H., et al., 2019. Source rocks evaluation of the paleogene Shahejie 3 Formation in the Dongpu depression, Bohai Bay Basin. Energy Explor. Exploit. 37 (1), 394–411. https://doi.org/10.1177/0144598718802447.

Kuske, S., Horsfield, B., Jweda, J., et al., 2019. Geochemical factors controlling the phase behavior of Eagle Ford Shale petroleum fluids. AAPG Bull. 103 (4), 835–870. https://doi.org/10.1306/09051817227.

Lee, K., Moridis, G.J., Ehlig-Economides, C.A., 2016. A comprehensive simulation model of kerogen pyrolysis for the in-situ upgrading of oil shales. SPE J. 21 (5), 1612–1630. https://doi.org/10.2118/173299-PA.

Li, W., Zhu, Y., 2014. Hydrocarbon generation characteristics and kinetic analysis of vitrinite of various coal ranks during thermal cracking in two thermal simulation systems. Energy Sources, Part A. 36 (15), 1650–1658. https://doi.org/10.1080/15567036.2013.831146.

Li, L., Zuo, Y.H., Tang, S.H., et al., 2016. Cenozoic thermal history of the Dongpu sag, Bohai Bay Basin. Geol. Explor. 3, 594–600.

Ma, B.J., Qi, J.F., Yu, F.S., 2017. An analysis of physical modeling of tectonic deformation in Dongpu sag. Acta Geosci. Sin. 38 (3), 430–438. https://doi.org/10.3975/cagsb.2017.03.13.

Moattari, M., Rabbani, A.R., Mahdavifar, Y., 2012. Estimating and optimizing the amount of generated hydrocarbon by determining kinetic parameters (A, E) in Pabdeh, Gurpi, and Kazhdumi source rocks with an open pyrolysis system. Petrol. Sci. Technol. 30 (22), 2306–2315. https://doi.org/10.1080/10916466.2010.511380.

Ni, Y., Ma, Q., Ellis, G.S., et al., 2011. Fundamental studies on kinetic isotope effect (KIE.of hydrogen isotope fractionation in natural gas systems. Geochem. Cosmochim. Acta 75 (10), 2696–2707. https://doi.org/10.1016/j.gca.2011.02.016.

Pepper, A.S., Corvi, P.J., 1995. Simple kinetic models of petroleum formation. Part I:

oil and gas generation from kerogen. Mar. Petrol. Geol. 12 (3), 291–319.
Peters, K.E., Burnham, A.K., Walters, C.C., 2015. Petroleum generation kinetics: single versus multiple heating ramp open-system pyrolysis. AAPG Bull. 99 (4), 591–616. https://doi.org/10.1306/11141414080.
Saad, A., Theis, S., Mohamed, M., 2020. Effect of kerogen thermal maturity on methane adsorption capacity: a molecular modeling approach. Molecules 25 (16), E3764. https://doi.org/10.3390/molecules25163764.
Schenka, H.J., Dieckmannb, V., 2004. Prediction of petroleum formation: the influence of laboratory heating rates on kinetic parameters and geological extrapolations. Mar. Petrol. Geol. 21, 79–95. https://doi.org/10.1016/j.marpetgeo.2003.11.004.
Shao, X.H., Pang, X.Q., Li, M.W., et al., 2020. Hydrocarbon retention in lacustrine shales during thermal maturation: insights from semi-open system pyrolysis. J. Petrol. Sci. Eng. 184, 106480. https://doi.org/10.1016/j.petrol.2019.106480.
Tang, S.L., Zuo, Y.H., Wu, W.T., et al., 2016. Thermal history and source rock thermal evolution history in the Qianliyuan subsag, Dongpu sag. Open J. Nat. Sci. 4 (4), 401–411.
Tang, X.Y., Zuo, Y.H., Kohn, B., et al., 2019. Cenozoic thermal history reconstruction of the Dongpu Sag, Bohai Bay Basin: insights from apatite fission-track thermochronology. Terra. Nova 31, 159–168. https://doi.org/10.1111/ter.12379.
Tissot, B.P., Pelet, R., Ungerer, P.H., 1987. Thermal history of sedimentary basins, maturation Indices, and kinetics of oil and gas generation. AAPG Bull. 71 (12), 1445–1466. https://doi.org/10.1306/703C80E7-1707-11D7-8645000102C1865D.
Ungerer, P., Pelet, R., 1987. Extrapolation of the kinetics of oil and gas formation from laboratory experiments to sedimentary basins. Nature 327 (6117), 52–54. https://doi.org/10.1038/327052a0.
Wang, M., Lu, S.F., Xue, H.T., et al., 2011. Hydrocarbon generation kinetic characteristics from different types of organic matter. Acta Geol. Sin. (Engl. Ed.). 85 (3), 702–711.
Wang, Z.X., Tang, Y.J., Wang, Y.L., et al., 2020. Kinetics of shale oil generation from kerogen in saline basin and its exploration significance: an example from the Eocene Qianjiang Formation, Jianghan Basin, China. J. Anal. Appl. Pyrolysis 150, 104885. https://doi.org/10.1016/j.jaap.2020.104885.
Yan, K.N., Zuo, Y.H., Yang, M.H., et al., 2019. Kerogen pyrolysis experiment and hydrocarbon generation kinetics in the Dongpu depression, Bohai Bay Basin, China. Energy Fuels 33 (9), 8511–8521. https://doi.org/10.1021/acs.energyfuels.9b02159.
Yousif, M., Wan, H.A., Habeeb, A., et al., 2019. Hydrocarbon generation potential of Oligocene oil shale deposit at onshore Penyu Basin, Chenor, Pahang, Malaysia. Energy Fuels 33 (1), 89–105. https://doi.org/10.1021/acs.energyfuels.8b03164.
Zuo, Y.H., Qiu, N.S., Zhang, Y., et al., 2011. Geothermal regime and hydrocarbon kitchen evolution of the offshore Bohai Bay Basin, North China. AAPG Bull. 95, 749–769. https://doi.org/10.1306/09271010079.
Zuo, Y.H., Qiu, N.S., Hao, Q.Q., et al., 2014. Present geothermal fields of the Dongpu sag in the Bohai Bay Basin. Acta Geol. Sin. (Engl. Ed.). 88 (3), 915–930.
Zuo, Y.H., Qiu, N.S., Hao, Q.Q., et al., 2015. Geothermal regime and source rock thermal evolution history in the Chagan sag, Inner Mongolia, northern China. Mar. Petrol. Geol. 59, 245–267. https://doi.org/10.1016/j.marpetgeo.2014.09.001.
Zuo, Y.H., Wang, C.C., Tang, S.L., et al., 2016. Mesozoic and Cenozoic thermal history and source rock thermal evolution of the Baiyinchagan sag, Erlian Basin, Northern China. J. Petrol. Sci. Eng. 139, 171–184. https://doi.org/10.1016/j.petrol.2015.12.025.
Zuo, Y.H., Yang, M.H., Hao, Q.Q., et al., 2020a. New progress on hydrocarbon-generation history of the Dongpu Depression in the Bohai Bay Basin based on thermal history and hydrocarbon generation kinetics. Acta Geol. Sin. (Engl. Ed.). 94 (5), 1724–1725. https://doi.org/10.1111/1755-6724.14576.
Zuo, Y.H., Jiang, S., Wu, S.H., et al., 2020b. Terrestrial heat flow and lithospheric thermal structure in the Chagan Depression of the Yingen-Ejinaqi Basin, north central China. Basin Res. 32 (6), 1328–1346. https://doi.org/10.1111/bre.12430.
Zuo, Y.H., Ye, B., Wu, W.T., et al., 2017. Present temperature field and cenozoic thermal history in the Dongpu depression, Bohai Bay Basin, north China. Mar. Petrol. Geol. 88, 696–711. https://doi.org/10.1016/j.marpetgeo.2017.08.037.
Zheng, Y.J., Jiang, C.Q., Liao, Y.H., 2021. Relationship between hydrocarbon gas generation and kerogen structural evolution revealed by closed system pyrolysis and quantitative Py-GC analysis of a type II kerogen. Energy Fuels 35 (1), 251–263. https://doi.org/10.1021/acs.energyfuels.0c02468.